nature neuroscience

Preferential encoding of visual categories in parietal cortex compared with prefrontal cortex

Sruthi K Swaminathan & David J Freedman

The ability to recognize the behavioral relevance, or category membership, of sensory stimuli is critical for interpreting the meaning of events in our environment. Neurophysiological studies of visual categorization have found categorical representations of stimuli in prefrontal cortex (PFC), an area that is closely associated with cognitive and executive functions. Recent studies have also identified neuronal category signals in parietal areas that are typically associated with visual-spatial processing. It has been proposed that category-related signals in parietal cortex and other visual areas may result from 'top-down' feedback from PFC. We directly compared neuronal activity in the lateral intraparietal (LIP) area and PFC in monkeys performing a visual motion categorization task. We found that LIP showed stronger, more reliable and shorter latency category signals than PFC. These findings suggest that LIP is strongly involved in visual categorization and argue against the idea that parietal category signals arise as a result of feedback from PFC during this task.

The ability to make binary categorical decisions about continuously varying sensory stimuli, such as whether a piece of fruit is ripe or unripe, or whether a baseball pitch is a ball or a strike, is critical for selecting appropriate behavioral responses and is observed in a wide range of animals, including insects[1], birds[2], non-human primates[2–5] and humans[6]. Neurophysiological studies have identified neuronal representations that reflect the category membership of stimuli[5,7,8] or abstract encoding of task rules[9] in the PFC, an area that is closely associated with higher cognitive and executive functions. Neuronal category[10,11] and rule signals[12] have also been observed in posterior parietal areas most often associated with visual-spatial processing related to attention and saccadic eye movements. In a recent study, monkeys were trained to group 360° of motion directions into two 180°-wide categories. After training, activity in LIP showed strong category encoding: neuronal responses were very similar for stimuli in the same category and differed sharply between stimuli in opposite categories. In contrast, neurons in the middle temporal (MT) area, an important motion processing area[13] that provides input to LIP[14], were strongly direction selective, but their activity did not reflect the learned categories.

How are feature representations in early visual areas transformed into abstract and experience-dependent representations such as those observed in LIP and PFC? It has been proposed that decisions about the category membership or abstract relevance of stimuli may be generated in PFC and that PFC could be a source for such representations observed in earlier visual areas[7,12,15–17], including LIP and inferior temporal cortex. Alternatively, category signals could be generated in brain areas, such as LIP, that are more closely connected with earlier sensory processing areas[14].

We directly compared the activity of LIP and PFC neurons in two monkeys trained to perform a visual category-matching task in which a set of continuously varying motion directions were divided into two categories by a learned category boundary. We found that, although both areas showed a clear and significant encoding of the learned categories, category effects in LIP were stronger, more reliable and appeared with a shorter latency than those in PFC. Furthermore, LIP showed a closer coupling with the monkeys' trial-by-trial decisions about the category of 'ambiguous' stimuli with directions on the category boundary. Together, these results suggest that LIP category signals are unlikely to originate in PFC during this task and that parietal cortex is highly involved in visual categorization and category-based decision making.

RESULTS

Delayed match-to-category task

We trained two monkeys to group 360° of motion directions into two categories defined by a learned category boundary[10] (**Fig. 1a**). During neurophysiological recordings, six evenly spaced (60° between directions) motion directions were used as sample and test stimuli, as well as two directions that were on the category boundary and had ambiguous category membership (**Fig. 1a**). Monkeys performed a delayed match-to-category (DMC) task (**Fig. 1b**) in which a sample stimulus (650 ms) was followed by a memory delay (1,000 ms) and a test stimulus (650 ms). The monkeys had to release a manual touch bar if the test was a category match to the sample. If the test was a non-match (on 50% of trials), it was followed by an additional delay (150 ms) and a second test stimulus (650 ms) that was always a category match to the sample and required a lever release. Some of the advantages of this task are that the monkeys' motor responses indicated 'match' and were not rigidly associated with either category, and the responses could not be planned until the appearance of the test stimulus.

During recordings, the monkeys correctly categorized each of the six directions of sample stimuli with greater than 90% accuracy and performed at chance (50%) for the two directions that were on the

Department of Neurobiology, The University of Chicago, Chicago, Illinois, USA. Correspondence should be addressed to D.J.F. (dfreedman@uchicago.edu).

Received 21 September 2011; accepted 17 November 2011; published online 15 January 2012; doi:10.1038/nn.3016

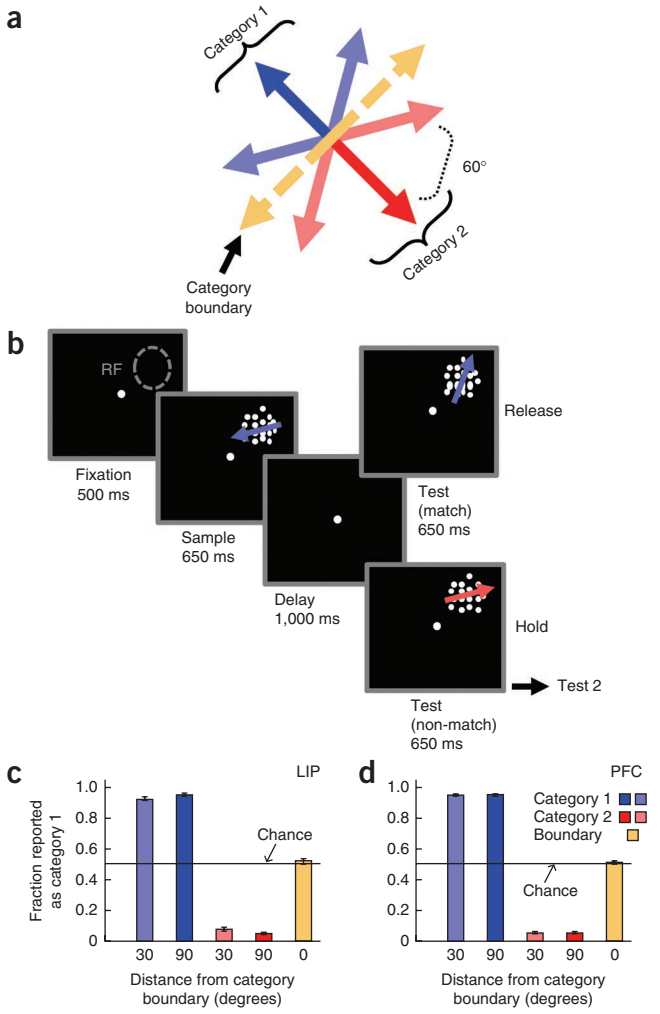

Figure 1 DMC task. (**a**) Monkeys grouped six motion directions into two categories (corresponding to the red and blue arrows) separated by a learned category boundary. Two additional directions were shown as sample stimuli that were on the category boundary and had ambiguous category membership (the two dashed yellow arrows). (**b**) Monkeys performed a DMC task and had to indicate (by releasing a lever) whether sample and test stimuli were in the same category. RF indicates the position of a neuron's receptive field. (**c**,**d**) The monkeys' average categorization performance (proportion of directions classified as category 1) during LIP (**c**) and PFC (**d**) recordings is shown as a function of distance from the category boundary. Error bars indicate s.e.m.

category boundary (**Fig. 1c**,**d**). The monkeys' accuracies and reaction times were very similar for the two categories and during LIP and PFC recordings sessions (**Table 1** and **Fig. 1c**,**d**). We conducted LIP and PFC recordings after the monkeys were fully trained and interleaved recording sessions from the two areas (see **Supplementary Note**). Thus, any differences between LIP and PFC activity are unlikely to be related to differences in behavioral performance or the amount of training.

Comparing neuronal category selectivity in LIP and PFC

We recorded from 76 LIP (monkey B, $n = 32$; monkey J, $n = 44$) and 447 PFC (monkey B, $n = 205$; monkey J, $n = 242$) neurons during DMC task performance (see also **Supplementary Fig. 1**). Many neurons showed activity that reflected the learned categories in both LIP (number of category selective neurons: sample, $n = 44$ of 76; delay, $n = 50$ of 76; test, $n = 42$ of 76) and PFC (sample, $n = 90$ of 447; delay, $n = 89$ of 447; test, $n = 84$ of 447) according to an unpaired t test ($P < 0.01$) that compared activity to the two categories, and the fraction of selective neurons was greater in LIP than PFC in all three of the task epochs (χ^2 test, $P < 0.0001$ in all epochs). Many neurons in both areas showed binary-like category selectivity in that they responded strongly and uniformly to the three directions in their preferred category and had uniformly weaker responses to directions in the nonpreferred category (**Fig. 2**).

The strength and reliability of neuronal category encoding were quantified using two complementary techniques. The first was a receiver-operating characteristic (ROC)-based analysis that, for each neuron, measured the degree of overlap in neuronal responses to the two categories across all trials (see Online Methods). ROC values could vary from 1.0 (very strong selectivity) to 0.5 (no selectivity) and indicate the reliability with which an ideal observer could read out category information given a neuron's firing rate on a single trial. Average fixation period ROC values greater than 0.5 are expected because raw ROC values (which can vary from 0.0 to 1.0) are rectified about 0.5, and this does not indicate any neuronal bias or anticipatory category signals (see Online Methods). The second technique was a category-tuning index (CTI) that tested the influence of the category boundary on average neuronal firing rates (averaged across trials for each direction) by computing the difference in firing rates between pairs of directions that are in the same versus different categories[5,10,17] (see Online Methods). The CTI can vary from 1.0 (strong category selectivity) to −1.0 (no activity difference between categories and a large difference within categories) and indicates the difference in firing rate between versus within categories, but does not measure the reliability of neuronal category effects.

Table 1 Behavioral performance of each monkey during LIP and PFC recordings

	Monkey B	Monkey J
Accuracy LIP (% correct)	93 ± 5	96 ± 4
Accuracy PFC (% correct)	92 ± 4	97 ± 3
Reaction time LIP	237 ± 31 ms	287 ± 42 ms
Reaction time PFC	225 ± 30 ms	281 ± 44 ms

Accuracy does not include on-boundary directions and excludes fixation breaks. Reaction times are shown for correct trials in which test stimulus #1 was a category match. Values are mean ± s.d.

Because a different proportion of neurons in LIP and PFC were category selective, we focused the analysis on neuronal populations in each area that were selected by a common criterion: neurons that differentiated among the six sample directions during the sample, delay and/or test epochs according to one-way analysis of variance (ANOVA comparing responses to the six directions) at $P < 0.01$ (see **Table 2**). ROC and CTI values were significantly greater in all three task epochs compared with the same neurons during the fixation epoch in LIP (paired t test, $P < 0.0005$ in all three epochs; **Fig. 3**) and PFC (paired t test, $P < 10^{-7}$ in all three epochs; **Fig. 3**). Furthermore, category selectivity was significantly stronger in LIP than in PFC during all three task epochs, as determined by ROC analysis (LIP versus PFC Wilcoxon rank sum test, sample, $P = 0.005$; delay, $P = 0.018$; test, $P = 0.002$; **Fig. 3a** and **Supplementary Fig. 2**). This suggests that the strength of category encoding, in terms of the ability to read out the sample category from neuronal activity on a trial-by-trial basis, is significantly stronger in LIP than in PFC. The CTI also revealed significantly stronger category selectivity in LIP than in PFC during the test epoch (rank sum test, $P = 0.003$; **Fig. 3b** and **Supplementary Fig. 3**)

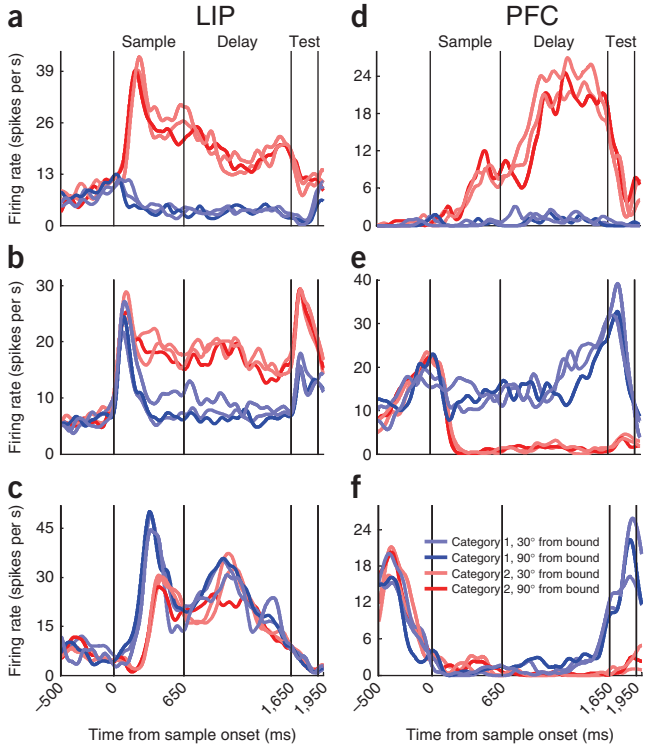

Figure 2 Examples of category-selective LIP and PFC neurons. (**a**–**f**) The responses of three LIP (**a**–**c**) and three PFC (**d**–**f**) neurons are shown. The red and blue traces indicate the three directions in category 1 and category 2, respectively. The pale red and blue traces represent directions closer to the category boundary, and the dark traces represent directions in the center of each category. Each neuron showed a tendency for strong selectivity for sample category during the sample, delay and/or test epochs. Data is shown only for correct trials.

and a nonsignificant trend toward stronger selectivity in LIP than in PFC during the sample (rank sum test, $P = 0.296$) and delay (rank sum test, $P = 0.124$).

Comparing the timing of category signals in LIP and PFC

We examined the time course of category selectivity in each brain area using 'sliding' versions of the ROC and CTI (see Online Methods) applied to the neural populations that were direction selective (one-way ANOVA across the six sample directions, $P < 0.01$) in the sample, delay and/or test epochs (LIP, $n = 67$ of 76; PFC, $n = 155$ of 447). Notably, both selectivity measures revealed that category selectivity appeared with a shorter latency in LIP than PFC following the onset of the sample stimulus (**Fig. 4**). We quantified the latency of category selectivity for each LIP and PFC neuron by evaluating the time at which the ROC or CTI crossed an arbitrary threshold (3.0 s.d. above the mean value during the fixation epoch for two consecutive time bins) in the early sample period (the initial 500 ms of sample presentation, see Online Methods). Across all neurons for which a latency was defined (that is, the selectivity threshold was crossed at some point during the early sample period), category selectivity emerged significantly earlier in LIP (ROC, mean = 112 ms; CTI, mean = 153 ms) than in PFC (ROC, mean = 185 ms; CTI, mean = 226 ms) according to a Wilcoxon rank sum test (ROC, $P = 0.00001$; CTI, $P = 0.002$; **Fig. 4**).

One concern is that the observed latency difference between LIP and PFC could be related to differences in the strength of category selectivity or firing rates between the two areas (see **Supplementary Fig. 4**). For example, neurons with higher firing rates or stronger selectivity might have shorter latency effects. However, this seemed unlikely in our experiments, as neurons with weak selectivity or low firing rates sometimes showed short-latency selectivity, and vice versa (**Fig. 4e**–**h** and **Supplementary Fig. 5**). To examine this issue directly, we employed a general linear model to conduct an analysis of covariance (ANCOVA). This approach allows the statistical significance of an effect of interest (for example, the difference in latency between LIP and PFC) to be determined while accounting for the variance from multiple co-varying factors (for example, strength of category selectivity and firing rate of each neuron). We applied the ANCOVA separately to both the ROC and CTI latency results (that is, the same results and neuronal populations shown in **Fig. 4b**,**d**) and found that in both cases there was a significant main effect of brain area (ANCOVA with latency as the dependent variable and selectivity strength and firing rate as covariates, LIP versus PFC, ROC, $P = 0.0039$; CTI, $P = 0.0052$), indicating that the difference in latency between LIP and PFC is very unlikely to be related to differences in firing rate or selectivity strength. We obtained similar results using a different analysis approach in which we compared the latencies of neuronal subpopulations with equal firing rates or strengths of selectivity (see **Supplementary Fig. 6** and **Supplementary Note**).

Table 2 Incidence of direction selectivity and category selectivity in PFC and LIP

	Sample	Delay	Test	Any epoch
LIP ($n = 76$)				
Direction selective (one-way ANOVA across six directions)	54 (71%)	50 (66%)	33 (43%)	67 (88%)
Category selective (t test, category 1 versus category 2)	44 (58%)	50 (66%)	42 (55%)	66 (87%)
PFC ($n = 447$)				
Direction selective (one-way ANOVA across six directions)	87 (19%)	84 (19%)	65 (15%)	155 (35%)
Category selective (t test, category 1 versus category 2)	90 (20%)	89 (20%)	84 (19%)	174 (39%)

The values above indicate the number (or percentage) of neurons significant at $P < 0.01$.

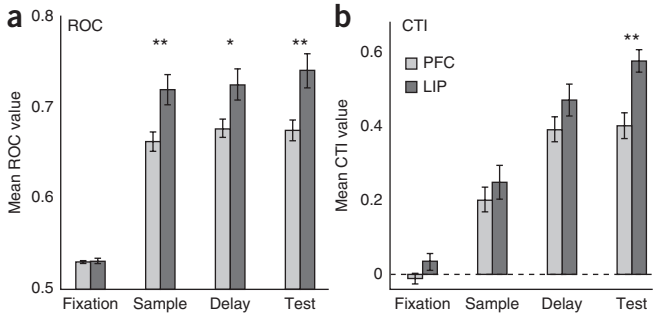

Figure 3 Strength of category selectivity across LIP and PFC populations. (**a**,**b**) The strength of category selectivity was measured using ROC (**a**) and CTI (**b**) analyses. ROC values for individual neurons could vary from 0.5 to 1.0. Average fixation period ROC values greater than 0.5 are expected because raw ROC values (which can vary from 0.0 to 1.0) are rectified about 0.5, and this does not indicate any neuronal bias or anticipatory category signals (see Online Methods). CTI values could vary from −1.0 to 1.0. For both measures, greater positive values indicate stronger category selectivity and mean values are shown for LIP (dark gray) and PFC (light gray) across all direction-selective (according to one-way ANOVA) neurons in each epoch. During the fixation epoch, ROC and CTI values are shown for neurons that were direction selective in any epoch. Error bars indicate the s.e.m. $^*P < 0.05$, $^{**}P < 0.01$, t test, LIP versus PFC.

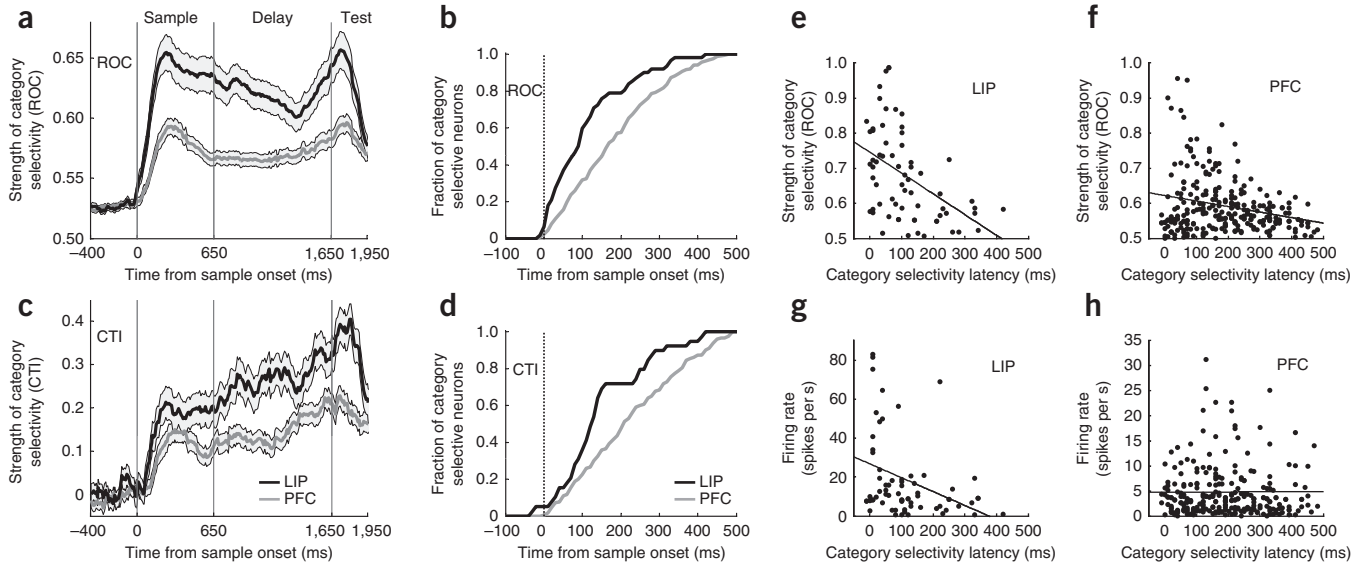

Figure 4 Time course of LIP and PFC category selectivity. (**a**,**c**) The time course of category selectivity across direction-selective LIP and PFC populations was determined by sliding ROC (**a**) and CTI (**c**) analyses. The shaded gray area around the solid traces (the mean ROC or CTI value) indicates the s.e.m. Average fixation period ROC values greater than 0.5 are expected because raw ROC values (which can vary from 0 to 1.0) are rectified about 0.5, and this does not indicate any neuronal bias or anticipatory category signals (see Online Methods). (**b**,**d**) Cumulative latency distributions across all neurons that showed significant category selectivity before 500 ms after sample onset according to ROC (LIP, $n = 62$; PFC, $n = 243$; **b**) and CTI (LIP, $n = 39$; PFC, $n = 181$; **d**) analyses revealed the fraction of LIP and PFC neurons that had become category selective by each time point. (**e**,**f**) Scatter plots show the relationship between category-selectivity strength and category-selectivity latency for LIP (**e**) and PFC (**f**) neurons. (**g**,**h**) Scatter plots show the relationship between firing rate and category-selectivity latency for LIP (**g**) and PFC (**h**) neurons. For **e**–**h**, linear regression fits are indicated by the dashed line.

Decision-related responses to ambiguous stimuli

We determined whether neuronal category representations can reflect the monkeys' trial-by-trial categorization decisions about stimuli with ambiguous category membership by examining the responses of 66 LIP and 324 PFC neurons that were tested with two sample directions that were on the category boundary (**Fig. 1a**; see Online Methods and **Supplementary Note**). A number of neurons in LIP and PFC that were category selective for the non-ambiguous sample directions also reflected the monkeys' classifications of the ambiguous sample directions (**Fig. 5a**–**d**).

Category signals for the ambiguous stimuli were, on average, stronger and more consistent in LIP than in PFC. For each neuron that was direction selective (ANOVA on six sample directions, $P < 0.01$) in each epoch in non-ambiguous trials, we calculated the category 1 versus category 2 ROC value on ambiguous trials (sorted according to the monkeys' behavioral report on each trial). ROC values near 0.0 and 1.0 indicate a strong preference for category 1 and category 2, respectively. We then separated neurons by whether they preferred category 1 or category 2 in non-ambiguous trials to determine whether they showed consistent category preferences in ambiguous and non-ambiguous trials (**Fig. 5e**,**f**). Across the population, LIP showed strong and reliable category selectivity for the ambiguous stimuli that agreed with neurons' category preferences for non-ambiguous directions during the sample (mean ROC value: category 1 = 0.45, category 2 = 0.53; t test, $P = 0.031$; **Fig. 5e**) and delay (category 1 = 0.43, category 2 = 0.60; t test, $P = 0.000016$) epochs, as well as a nonsignificant trend in the test (category 1 = 0.48, category 2 = 0.60; t test, $P = 0.058$) epoch. In contrast, the PFC population showed only a weak and nonsignificant trend toward reflecting the monkeys' classifications of ambiguous stimuli during the sample (mean ROC value: category 1 = 0.48, category 2 = 0.50; category 1 versus category 2, t test, $P = 0.251$; **Fig. 5f**), delay (category 1 = 0.49, category 2 = 0.51;

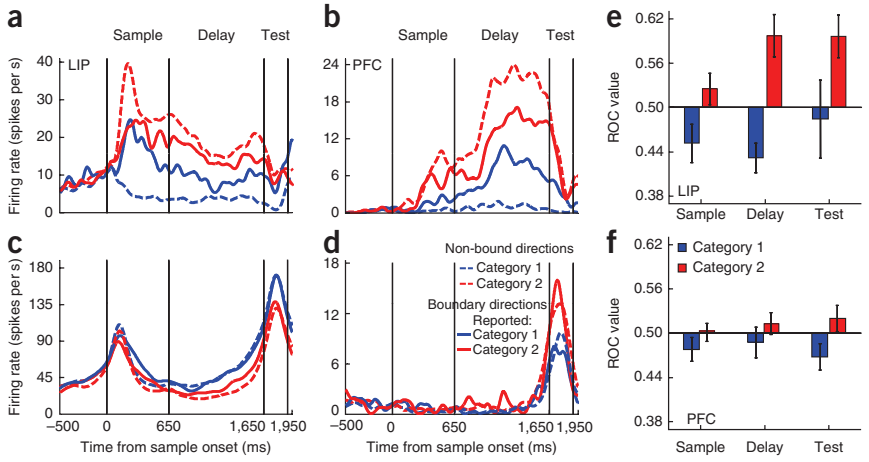

Figure 5 Neuronal activity to on-boundary directions with ambiguous category membership. (**a**–**d**) Examples of single LIP (**a**,**c**) and PFC (**b**,**d**) neurons to ambiguous sample directions (solid red and blue traces, activity sorted according to monkeys' reports of category membership on each trial) and non-ambiguous directions (dashed red and blue traces, activity averaged across the three directions in each category). (**e**,**f**) Population average category selectivity values (ROC) on ambiguous trials are shown for LIP (**e**) and PFC (**f**). Neurons were sorted according to whether they preferred category 1 (blue) or category 2 (red) in non-ambiguous trials. ROC values of 0 and 1.0 indicate strong selectivity for categories 1 and 2, respectively. Error bars represent s.e.m.

t test, $P = 0.296$) and test (category 1 = 0.47, category 2 = 0.52; *t* test, $P = 0.058$) epochs (**Supplementary Fig. 7**).

ROC values on ambiguous trials were also computed as a percentage of those observed on non-ambiguous trials. Across the same populations (**Fig. 5e**,**f**), ROC value percentages were greater in LIP than in PFC during the sample (LIP, 18.4%; PFC, 8.9%), delay (LIP, 39.4%; PFC, 7.1%) and test (LIP, 22.5%; PFC, 14.2%) epochs. Thus, in addition to showing stronger and shorter latency category selectivity, LIP also shows a more reliable encoding of the monkeys' trial-by-trial classifications of ambiguous stimuli.

DISCUSSION

Prior work found that activity in area MT, a cortical area that is critically involved in visual motion processing[13] and directly interconnected with LIP[14], showed strong direction tuning during the DMC task, but did not exhibit an obvious influence of the learned categories[10]. We sought to understand how basic visual feature representations, such as those in area MT, are transformed by learning into more abstract representations, as have been observed in LIP and PFC. Our findings regarding the timing, strength and reliability of category selectivity suggest that category signals in LIP during the motion-DMC task are unlikely to arise via top-down inputs from PFC. One possibility is that direction tuning in area MT is transformed into category tuning in LIP by learning-dependent changes in the direct synaptic connections between area MT and LIP[10,18]. Alternatively, this transformation may involve multiple interconnected processing stages in and around the parietal cortex, including the medial superior temporal[19], ventral intraparietal[20,21] and 7a (refs. 12,22) areas. Thus, additional studies will be needed to understand the relative roles of LIP and other interconnected parietal areas.

Studies of visual-shape categorization compared activity in PFC and inferior temporal cortex (ITC) and found stronger category signals in PFC, while ITC neurons typically showed stronger shape and/or feature tuning and much weaker category effects. As we observed in both PFC and LIP, many PFC neurons in our prior shape-categorization studies showed strong category selectivity that was almost binary. In contrast, even the ITC neurons that showed the strongest category selectivity also showed a greater degree of variability among stimuli in each category, consistent with neurons showing an influence of both the category boundary and tuning for stimulus features[7]. ITC only showed strong binary-like category signals about the sample stimulus during the test period, which was very late in the trial (>1.0 s following sample onset)[7]. Together, these results suggest that ITC is unlikely to be a source for such category signals to PFC and other areas.

As our neuronal recordings were conducted once the monkeys were fully trained, the roles of LIP and PFC during the learning process remain unclear. One possibility is that PFC may be more involved during earlier stages of categorization training and that strong category effects in LIP might emerge only after the monkeys have completed the learning process. This is consistent with the idea that, as a task becomes more practiced and familiar, neuronal activation migrates away from areas that are more involved in executive control (such as PFC) and toward more posterior cortical areas (such as parietal or premotor cortex) or subcortical structures as task performance becomes less effortful and more automatic. However, a previous study found that strong category effects in LIP were evident after only 2–3 weeks of training on the motion-DMC task[10], suggesting that extremely long training durations (for example, more than 2 weeks) are not required to observe LIP category signals. Whether category signals could develop over shorter time scales (for example, in a single training session) remains to be determined.

A related question concerns the roles of LIP and PFC during tasks using variable decision criteria or category boundaries. Such tasks are known to rely on PFC[23], and studies using more dynamic tasks have found strong category or rule signals in PFC[9,24] and the frontal eye fields[8], which closely track the monkeys' rapidly changing decision criteria. Although LIP has not been directly tested during more dynamic categorization tasks, it is likely that LIP would reflect rapidly changing task rules or decision criteria for two reasons. First, our finding that LIP showed a stronger coupling than PFC with the monkeys' trial-by-trial decisions about the category of ambiguous boundary-sample stimuli (**Fig. 5**) suggests that LIP direction tuning is not fixed and can reflect the monkeys' changing decision criteria. Second, a previous study[12] found that parietal activity reflects the rule required to solve a visual discrimination task when the rule is varied from trial to trial.

The strength of category signals in LIP and the fact that they were observed in a majority of neurons raise questions about their relationship with well-known signals in LIP for spatial attention[25] and eye movements[26]. Recent work has implicated the parietal cortex (including area LIP) in nonspatial cognitive processing[10,12,27,28], and one study found that category signals are observed even when stimuli are presented outside LIP neurons' receptive fields[17], suggesting an independent encoding of spatial and nonspatial factors. However, it is unclear how spatial and nonspatial signals are combined in LIP and read-out by downstream areas.

It will also be important to understand the relationship between the neuronal category signals that we observed and those that have been observed during other types of categorization and decision-making tasks. Category signals may be just one example of a more general 'abstract framework' for decision making between discrete alternatives[29]. If so, neuronal category tuning might be closely related to decision-related signals that have been observed in LIP during perceptual-decision tasks[30], which might not be necessarily tied to specific motor plans[31]. Finally, the generalized nature of LIP category encoding was underscored by recent findings that LIP neurons often encoded both motion-category signals and reflected the learned pairings between associated shapes[11]. The shape-pair and motion-category signals that were previously observed in LIP appeared with a similar strength and time course, suggesting that LIP's role in visual categorization extends to tasks using both spatial and nonspatial visual stimuli. Together, these results suggest that parietal cortex, and LIP in particular, is an important processing stage for visual categorization and category-based decision making.

METHODS

Methods and any associated references are available in the online version of the paper at http://www.nature.com/natureneuroscience/.

Note: Supplementary information is available on the Nature Neuroscience website.

ACKNOWLEDGMENTS

We thank S. McClellan for animal training and technical assistance, G. Huang, C. Rishel and S. Thomas for technical assistance, and the staff of The University of Chicago Animal Resources Center for expert veterinary assistance. We also thank J. Assad, J. Fitzgerald, T. Herrington, G. Ibos, J. McKee, E. Miller, C. Pack, M. Riesenhuber and A. Sarma for helpful discussions and/or comments on an earlier version of this manuscript. This work was supported by US National Institutes of Health grant R01 EY019041. Additional support was provided by a National Science Foundation Faculty Early Career Development Award, the Alfred P. Sloan Foundation, the Brain Research Foundation and US National Institutes of Health Training Grant 5T32GM007839.

AUTHOR CONTRIBUTIONS

D.J.F. and S.K.S. designed the experiments, analyzed the data and wrote the manuscript. S.K.S. trained the monkeys and performed all neurophysiological recordings. D.J.F. assisted in monkey training and neurophysiological recordings.

COMPETING FINANCIAL INTERESTS
The authors declare no competing financial interests.

Published online at http://www.nature.com/natureneuroscience/.
Reprints and permissions information is available online at http://www.nature.com/reprints/index.html.

1. Wyttenbach, R.A., May, M.L. & Hoy, R.R. Categorical perception of sound frequency by crickets. *Science* **273**, 1542–1544 (1996).
2. Roberts, W.A. & Mazmanian, D.S. Concept learning at different levels of abstraction by pigeons, monkeys and people. *J. Exp. Psychol. Anim. Behav. Process.* **14**, 247–260 (1988).
3. Vogels, R. Categorization of complex visual images by rhesus monkeys. *Eur. J. Neurosci.* **11**, 1223–1238 (1999).
4. Fabre-Thorpe, M., Richard, G. & Thorpe, S.J. Rapid categorization of natural images by rhesus monkeys. *Neuroreport* **9**, 303–308 (1998).
5. Freedman, D.J., Riesenhuber, M., Poggio, T. & Miller, E.K. Categorical representation of visual stimuli in the primate prefrontal cortex. *Science* **291**, 312–316 (2001).
6. Ashby, F.G. & Maddox, W.T. Human category learning. *Annu. Rev. Psychol.* **56**, 149–178 (2005).
7. Freedman, D.J., Riesenhuber, M., Poggio, T. & Miller, E.K. A comparison of primate prefrontal and inferior temporal cortices during visual categorization. *J. Neurosci.* **23**, 5235–5246 (2003).
8. Ferrera, V.P., Yanike, M. & Cassanello, C. Frontal eye field neurons signal changes in decision criteria. *Nat. Neurosci.* **12**, 1458–1462 (2009).
9. Wallis, J.D., Anderson, K.C. & Miller, E.K. Single neurons in prefrontal cortex encode abstract rules. *Nature* **411**, 953–956 (2001).
10. Freedman, D.J. & Assad, J.A. Experience-dependent representation of visual categories in parietal cortex. *Nature* **443**, 85–88 (2006).
11. Fitzgerald, J.K., Freedman, D.J. & Assad, J.A. Generalized associative representations in parietal cortex. *Nat. Neurosci.* **14**, 1075–1079 (2011).
12. Stoet, G. & Snyder, L.H. Single neurons in posterior parietal cortex of monkeys encode cognitive set. *Neuron* **42**, 1003–1012 (2004).
13. Born, R.T. & Bradley, D.C. Structure and function of visual area MT. *Annu. Rev. Neurosci.* **28**, 157–189 (2005).
14. Lewis, J.W. & Van Essen, D.C. Corticocortical connections of visual, sensorimotor, and multimodal processing areas in the parietal lobe of the macaque monkey. *J. Comp. Neurol.* **428**, 112–137 (2000).
15. Jiang, X. *et al.* Categorization training results in shape- and category-selective human neural plasticity. *Neuron* **53**, 891–903 (2007).
16. Shadlen, M.N., Kiani, R., Hanks, T.D. & Churchland, A.K. Neurobiology of decision making: an intentional framework. in *Better Than Conscious? Decision Making, the Human Mind, and Implications for Institutions* (eds. Engel, C. & Singer, W.) 71–102 (MIT Press, Cambridge, Massachusetts, 2008).
17. Freedman, D.J. & Assad, J.A. Distinct encoding of spatial and nonspatial visual information in parietal cortex. *J. Neurosci.* **29**, 5671–5680 (2009).
18. Ferrera, V.P. & Grinband, J. Walk the line: parietal neurons respect category boundaries. *Nat. Neurosci.* **9**, 1207–1208 (2006).
19. Williams, Z.M., Elfar, J.C., Eskandar, E.N., Toth, L.J. & Assad, J.A. Parietal activity and the perceived direction of ambiguous apparent motion. *Nat. Neurosci.* **6**, 616–623 (2003).
20. Cook, E.P. & Maunsell, J.H. Attentional modulation of behavioral performance and neuronal responses in middle temporal and ventral intraparietal areas of macaque monkey. *J. Neurosci.* **22**, 1994–2004 (2002).
21. Nieder, A., Diester, I. & Tudusciuc, O. Temporal and spatial enumeration processes in the primate parietal cortex. *Science* **313**, 1431–1435 (2006).
22. Merchant, H., Crowe, D.A., Robertson, M.S., Fortes, A.F. & Georgopoulos, A.P. Top-down spatial categorization signal from prefrontal to posterior parietal cortex in the primate. *Front. Syst. Neurosci.* **5**, 69 (2011).
23. Miller, E.K. & Cohen, J.D. An integrative theory of prefrontal cortex function. *Annu. Rev. Neurosci.* **24**, 167–202 (2001).
24. Roy, J.E., Riesenhuber, M., Poggio, T. & Miller, E.K. Prefrontal cortex activity during flexible categorization. *J. Neurosci.* **30**, 8519–8528 (2010).
25. Bisley, J.W. & Goldberg, M.E. Attention, intention, and priority in the parietal lobe. *Annu. Rev. Neurosci.* **33**, 1–21 (2010).
26. Snyder, L.H., Batista, A.P. & Andersen, R.A. Intention-related activity in the posterior parietal cortex: a review. *Vision Res.* **40**, 1433–1441 (2000).
27. Gottlieb, J. & Snyder, L.H. Spatial and non-spatial functions of the parietal cortex. *Curr. Opin. Neurobiol.* **20**, 731–740 (2010).
28. Oristaglio, J., Schneider, D.M., Balan, P.F. & Gottlieb, J. Integration of visuospatial and effector information during symbolically cued limb movements in monkey lateral intraparietal area. *J. Neurosci.* **26**, 8310–8319 (2006).
29. Freedman, D.J. & Assad, J.A. A proposed common neural mechanisms for categorization and perceptual decisions. *Nat. Neurosci.* **14**, 143–146 (2011).
30. Gold, J.I. & Shadlen, M.N. The neural basis of decision making. *Annu. Rev. Neurosci.* **30**, 535–574 (2007).
31. Bennur, S. & Gold, J.I. Distinct representations of a perceptual decision and the associated oculomotor plan in the monkey lateral intraparietal area. *J. Neurosci.* **31**, 913–921 (2011).

ONLINE METHODS

Behavioral task and stimulus display. We trained monkeys to indicate whether a test stimulus was in the same category as a previously presented sample stimulus by releasing a lever. Stimuli were high-contrast, 9.0° diameter random dot movies composed of 190 dots per frame, which moved at 12° per s with 100% coherence, and were displayed at a frame rate of 75 frames per s. Monkeys maintained gaze fixation in a 2.0° radius of a fixation point. Identical stimuli, timings and rewards were used for PFC and LIP recordings and for the two monkeys.

Gaze positions were measured using an EyeLink 1000 optical eye tracker (SR Research) at a sampling rate of 1.0 kHz and stored for offline analysis. Monkeylogic software (http://www.monkeylogic.net/) was used to control task events, stimuli and rewards, and to monitor and store behavioral events[32]. Stimuli were displayed on a 21-inch color CRT monitor (1,280 × 1,024 resolution, 75 Hz, 57-cm viewing distance).

LIP and PFC recording sessions were interleaved in each monkey. In monkey J, 35 PFC recordings sessions were followed by 29 LIP sessions and an additional 15 PFC sessions. In monkey B, most LIP recordings (n = 22 sessions) were conducted first, followed by PFC recordings (n = 36 sessions) and simultaneous LIP-PFC recording sessions (n = 4 sessions). This recording sequence allowed for a comparison of early (pre-PFC) LIP data and late (post-PFC) LIP data to ensure that the patterns of neuronal responses and selectivity were stable across time.

During offline spike sorting, waveform signals corresponding to single units were identified and assigned a subjective score from 1–5, where 5 indicates unequivocal recordings from a single neuron and that not a single action potential was lost and no noise was included during the session, whereas 1 indicates that the unit is likely a single neuron, but significant interference from noise and waveforms from other neurons and loss of spikes has occurred. Only well-isolated single units were included in subsequent analysis (mean score: LIP, 3.9; PFC, 3.8; units with scores below 3.0 were not included in the population).

Electrophysiological recording. Two male monkeys (*Macaca mulatta*, 8.0–10.0 kg) were implanted with a headpost and two recording chambers. Stereotaxic coordinates for chamber placement were determined from magnetic resonance images (**Supplementary Fig. 1**). PFC chambers were centered on the principal sulcus and anterior to the arcuate sulcus, ~27.0 mm anterior to the intra-aural line. LIP chambers were positioned over the intraparietal sulcus (IPS) centered ~3.0 mm posterior to the intra-aural line. All procedures were in accordance with the University of Chicago's Animal Care and Use Committee and US National Institutes of Health guidelines.

LIP recordings were conducted using single 75-µm tungsten microelectrodes (FHC), a dura piercing guide tube, and a Kopf (David Kopf Instruments) hydraulic microdrive system. PFC recordings were made using 250-µm dura-piercing tungsten microelectrodes (FHC) and a custom manual microdrive system that allowed simultaneous recordings from up to 16 electrodes. Neurophysiological signals were amplified, digitized and stored for offline spike sorting (Plexon) to verify the quality and stability of neuronal isolations (see **Supplementary Note**). Recordings were usually made from either LIP or PFC, although simultaneous recordings from both areas were made on a subset (n = 5) of sessions.

Receptive field mapping and stimulus placement. PFC and IPS neurons were tested with a memory-saccade task. Most IPS (and some PFC) neurons were also tested with a sparse noise stimulus during passive fixation[10,17]. Neurons were considered to be in LIP if they showed spatially selective visual responses and/or delay activity during the memory-saccade task or were located between such neurons. Stimuli during the DMC task were always presented in LIP receptive fields. PFC and LIP neurons were not pre-screened for direction or category selectivity.

Slightly different approaches were used to map neurons' receptive fields in LIP and PFC in an effort to maximize neuronal responses during the DMC task. Responses during the memory-saccade and sparse noise tasks were analyzed in real time to estimate the position of LIP receptive fields and to guide DMC stimulus placement. The typical eccentricity of stimulus placement for LIP recordings was ~6.0–10.0°. PFC responses during the memory-saccade task were less effective in guiding DMC stimulus placement, as PFC responses are often highly task dependent[33]. For most PFC recordings (n = 55 of 86 sessions), sample and test stimuli were presented in blocks of 30 trials at three non-overlapping locations in the contralateral visual field centered 7.0° from fixation, which covered much of the contralateral visual field on the CRT. For the remaining PFC recording sessions (31 of 86), stimuli were shown at a single fixed location (7.0° from fixation along the horizontal axis in the contralateral visual field). For PFC data with stimuli shown at three locations, each neuron's receptive field was defined as the location (of the three) that elicited the greatest average firing rate during the sample and delay, and only trials with stimuli at that location were used for subsequent analyses. Similar results were observed using only the one-location or three-location PFC datasets, or using PFC data for which stimuli were presented at the worst of the three locations.

Boundary trial behavioral methods. On trials in which an on-boundary direction was shown as the sample, the first test stimulus was always chosen to be one of the two directions perpendicular to the boundary (in the center of each category), allowing the monkeys' categorization of the sample to be inferred by whether they responded to the first or second test stimulus. Monkeys were rewarded at chance for responding to test stimuli on boundary-sample trials. Monkeys performed at chance levels (50%) for the two ambiguous stimuli, and usually did not show large behavioral biases (that is, match or non-match biases). Sessions in which the monkeys did show large biases (>70%/30% or 30%/70% match/non-match) on the boundary trials were excluded from boundary trial analysis (n = 18 of 142 sessions discarded).

Data analysis. The patterns of behavioral and neuronal results were similar and all main effects were observed in both monkeys. Thus, the two datasets were combined for all population analyses. Firing rates were computed for each neuron in four time windows corresponding to the four phases of the task: fixation, sample, delay and test. The fixation epoch was a 500-ms window ending at sample onset. The sample epoch was a 650-ms window that began 80 ms after sample onset (to account for neuronal response latencies). The delay epoch was an 800-ms window that began 300 ms following sample offset, and the test epoch was 300 ms in duration, beginning at test onset. The test epoch was necessarily shorter, as the match trials ended with the monkey's lever release. For trials in which the sample was not on the category boundary, neuronal activity was analyzed only on correct trials. For the trials in which the sample direction was on the category boundary, we analyzed neuronal activity for both rewarded and non-rewarded trials provided the monkey successfully maintained fixation.

The strength and time course of category selectivity was evaluated using a ROC analysis[7,34,35] and a CTI. The ROC analysis was applied to the distribution of firing rates on each trial during each analysis epoch. The area under the ROC curve is a value between 0.0 and 1.0 indicating the performance of an ideal observer in assigning category membership based on each neuron's trial-by-trial firing rates. Values of 0.0 and 1.0 correspond to strong selectivity (non-overlapping responses) for categories 1 and 2, respectively. Values of 0.5 indicate complete overlap in the distributions of firing rates to the two categories (that is, no category selectivity). Raw ROC values were rectified about 0.5, yielding values that varied from 0.5 (no selectivity) to 1.0 (strong selectivity for either category). Average fixation period ROC values greater than 0.5 are expected because of this rectification operation (for example, a raw ROC value of 0.49 becomes 0.51 after the rectification), and this does not indicate any neuronal bias or anticipatory category signals. The CTI measured the difference in firing rate (averaged across all trials for each direction) for each neuron between pairs of directions in different categories (a between category difference) and the difference in activity between pairs of directions in the same category (a within category difference). The CTI was defined as the difference between the within category and between category differences divided by their sum. Values of the index could vary from +1.0 (strong binary-like differences in activity to directions in the two categories) to −1.0 (large activity differences between directions in the same category, no difference between categories). A CTI value of 0.0 indicates the same difference in firing rate between and within categories.

The time course of category selectivity was determined by computing the ROC or CTI using a 200-ms analysis window that was stepped in 10-ms intervals over the course of the trial. For each neuron, the latency of category selectivity was defined as the first time bin at which the mean fixation period ROC or CTI value was exceeded by 3.0 s.d. for two consecutive time bins before 500 ms of after sample onset. Similar results were observed with various latency thresholds, window widths and step sizes.

On each boundary sample trial, we inferred the monkeys' category assignment of the sample stimulus according to the category membership of the first test stimulus and whether the monkey released the lever during its presentation. Ambiguous sample trials were then divided into two groups according to

the monkeys' report about the sample category (see **Supplementary Note**). Each neuron's preferred category was determined by its average firing rate on non-ambiguous trials. To analyze the strength of category selectivity for the ambiguous sample trials, we focused on neurons that were direction selective (according to a one-way ANOVA across six directions at $P < 0.01$) on non-ambiguous trials. The raw ROC was computed separately for neurons that preferred category 1 or category 2 on non-ambiguous trials, giving ROC values that varied from 0.0 (strong selectivity for category 1) to 1.0 (strong selectivity for category 2). This analysis was applied separately to the sample, delay and test epochs.

ANCOVA. One of the assumptions of the ANCOVA is that the data being examined is normally distributed. Because the distributions of latencies, firing rates, and selectivity strengths were often not normally distributed, we employed the Box-Cox Power transformation on the data prior to computing the ANCOVA to satisfy this assumption. However, very similar (and statistically significant) results were observed in all cases without the Box-Cox transformation.

32. Asaad, W.F. & Eskandar, E.N. A flexible software tool for temporally-precise behavioral control in Matlab. *J. Neurosci. Methods* **174**, 245–258 (2008).
33. Asaad, W.F., Rainer, G. & Miller, E.K. Task-specific neural activity in the primate prefrontal cortex. *J. Neurophysiol.* **84**, 451–459 (2000).
34. Green, D.M. & Swets, J.A. *Signal Detection Theory and Psychophysics* (J. Wiley & Sons, New York, 1966).
35. Tolhurst, D.J., Movshon, J.A. & Dean, A.F. The statistical reliability of signals in single neurons in cat and monkey visual cortex. *Vision Res.* **23**, 775–785 (1983).

doi:10.1038/nn.3016

Preferential encoding of visual categories in parietal cortex compared to prefrontal cortex
Sruthi K. Swaminathan & David J. Freedman

Supplemental Note

Controls for strength versus latency of category selectivity. In comparing the latency of category selectivity between LIP and PFC, it is essential to ensure that the observed difference in latency is not primarily due to differences in the strength of category selectivity in the two areas. In fact, category selectivity (measured by the ROC) was stronger in LIP (mean index = 0.679) than PFC (mean index = 0.593) during the early sample (80-500 ms after sample onset) among all neurons that were included in the latency analysis (N = 62 LIP neurons, N = 243 PFC neurons). As described in the main manuscript, category selectivity across these populations of neurons was observed with a significantly shorter latency in LIP (mean = 112 ms) than PFC (mean = 185 ms) according to a Wilcoxon rank sum Test ($P < 0.001$). To ensure that the observed difference in latency was not due to the difference in selectivity strength, we compared subpopulations of LIP and PFC neurons that were matched in their selectivity strength. To identify matched populations, we eliminated the 26.6% of LIP neurons (N = 16 excluded, N = 46 remaining neurons) with the *strongest* selectivity values and also the 26.6% of PFC neurons (N = 65 excluded, N = 178 remaining neurons) with the *weakest* category selectivity index values. These subpopulations were very similar in their average strengths of category selectivity (LIP: mean index = 0.619; PFC: mean index = 0.619). Importantly, these matched populations also showed a significant difference in their category selectivity latencies (LIP: mean = 134 ms; PFC: mean = 181 ms; LIP vs. PFC Wilcoxon rank sum Test, $P = 0.008$) that was very similar to that observed across the entire population. The scatter plots in Supplemental Fig. 6a (LIP) and 6b (PFC) show the selectivity strength and latency of category selectivity across the population. The points in black indicate those neurons that were eliminated in the above analysis. The red points indicate the remaining neurons which had matched selectivity strength on average.

Among all neurons used in the latency analysis, we eliminated an identical percentage of neurons from PFC and LIP in 0.1% increments until the mean ROC value for the remaining PFC neurons was equal or greater than the mean ROC value for the remaining LIP neurons. We then excluded from subsequent analysis all PFC neurons that were *below* this threshold (neurons with

the lowest ROC values) and all LIP neurons that were *above* this threshold (neurons with the highest ROC values). This produced populations of PFC and LIP neurons that were matched in their average ROC values.

Controls for firing rate versus latency of category selectivity. We also examined whether the difference in latency between LIP and PFC was related to differences in neuronal firing rates. Firing rates during the early sample epoch (80-500 ms after sample onset) were stronger in LIP (mean = 18.78 Hz) than PFC (mean = 4.77 Hz) among all neurons that were included in the latency analysis (N = 62 LIP neurons, N = 243 PFC neurons). To ensure that the observed difference in latency was not due to the difference in firing rates, we compared subpopulations of LIP and PFC neurons that were matched in their average firing rate. To identify matched populations, we eliminated the 36.3% of LIP neurons (N = 23 excluded; N = 39 remaining neurons) with the *highest* firing rates and also the 36.3% of PFC neurons (N = 88 excluded; N = 155 remaining neurons) with the *lowest* firing rates. These subpopulations were very similar in their average firing rate (LIP: mean = 6.82 Hz; PFC: mean = 6.92 Hz). Importantly, they also showed a significant difference in the average latency of category selectivity (LIP: mean = 135 ms; PFC: mean = 181 ms; LIP vs. PFC Wilcoxon rank sum Test, P = 0.024) that was very similar to that observed across the entire population. The scatter plots in Supplemental Figs. 6c (LIP) and 6d (PFC) show the relationship between the firing rate and latency of category selectivity. The points in black indicate those neurons that were eliminated in the above analysis. The red points indicate the remaining neurons which had matched firing rates on average.

Among all neurons used in the latency analysis, we eliminated an identical percentage of neurons from PFC and LIP in 0.1% increments until the mean firing rate for the remaining PFC neurons was equal or greater than the mean firing rate for the remaining LIP neurons. We then excluded from subsequent analysis all PFC neurons that fell at or below this threshold (neurons with the lowest firing rates) and all LIP neurons that were at or above this threshold (neurons with the highest firing rates). This produced populations of PFC and LIP neurons that were matched in their average firing rate.

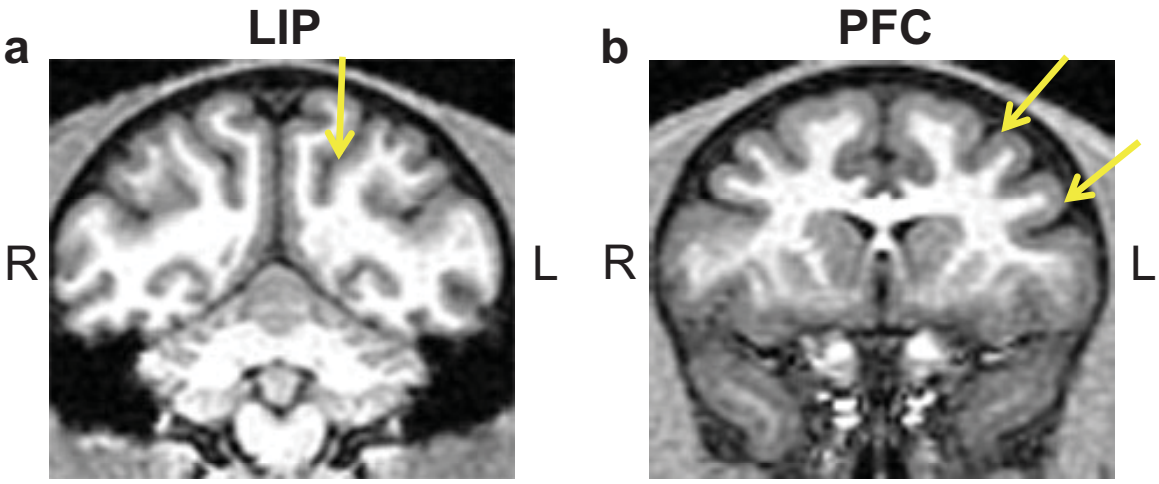

Figure S1. Recording Locations. Anatomical MRI images show approximate locations of LIP (a) and PFC (b) recordings as indicated by the superimposed yellow arrows. LIP recordings targeted the lateral bank of the intraparietal sulcus approximately 1.0-7.0 mm posterior to the intra-aural line. PFC recordings were accessed via chambers centered over the principal sulcus and anterior to the arcuate sulcus, approximately 27 mm anterior from the intra-aural line. PFC recordings were focused on the cortex between the two arrows.

Nature Neuroscience: doi:10.1038/nn.3016

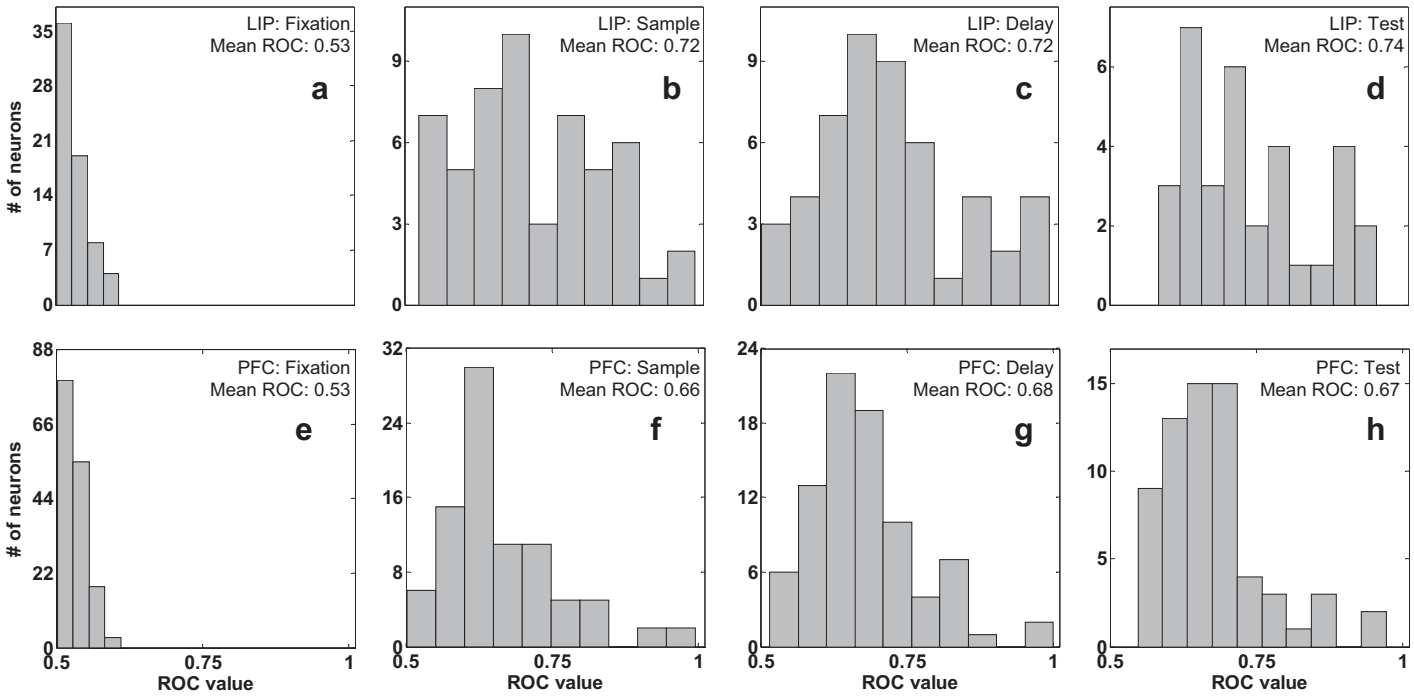

Figure S2. Distributions of ROC values across LIP and PFC populations. An ROC analysis measured the strength of category selectivity of individual neurons (see *Methods*). ROC values for individual neurons could vary from 0.5 (no selectivity) to 1.0 (perfect category selectivity). (a-h) The gray bars show index values across the population of direction selective (according to one-way ANOVA at $P < 0.01$) LIP (a-d) and PFC (e-h) neurons in each epoch. During the fixation epoch (a,e), ROC values are shown for all direction selective neurons (in any epoch).

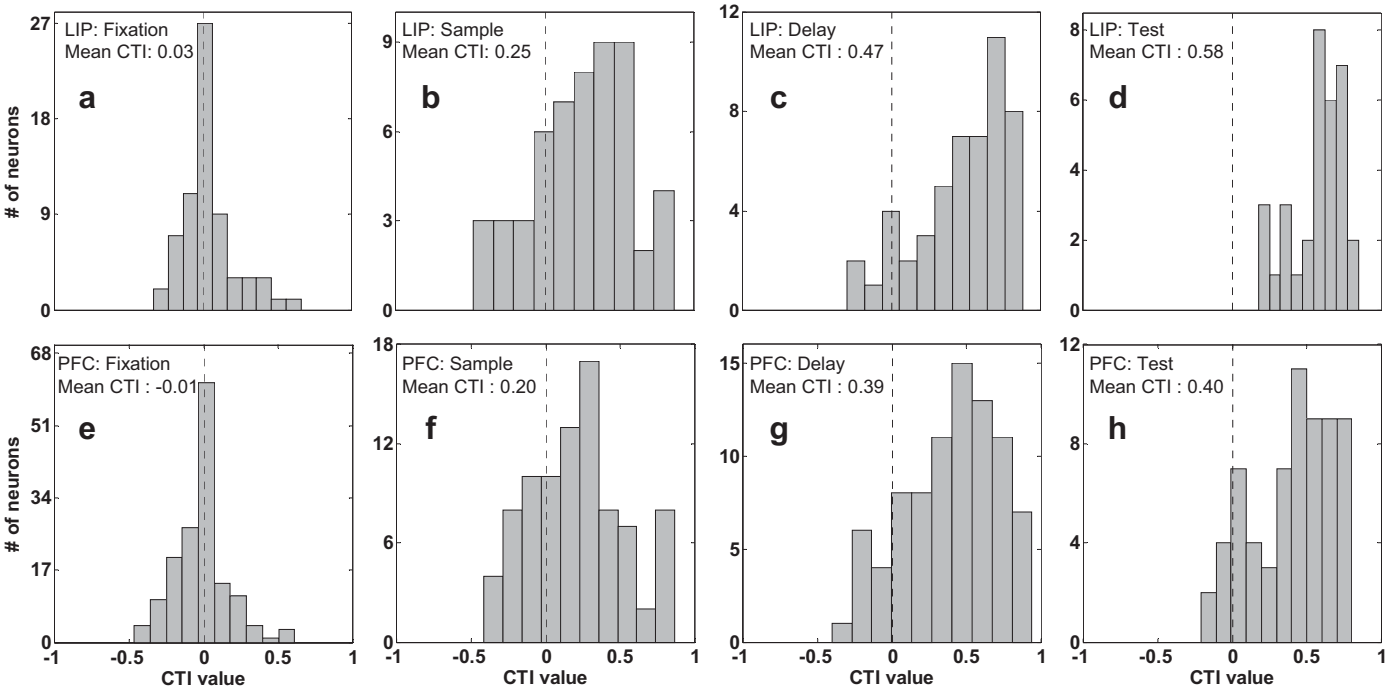

Figure S3. Distributions of category tuning index (CTI) values across LIP and PFC populations. A category tuning index was computed that measured the strength of category selectivity of individual neurons (see *Methods*). Positive values of the index indicate larger activity differences between categories and/or more similar activity within categories. The gray bars show index values across the populations of direction selective neurons (according to a one-way ANOVA at P<0.01) in LIP (a-d) and PFC (e-h) in each epoch. During the fixation epoch (a,e), CTI values are shown for all direction selective neurons (in any epoch).

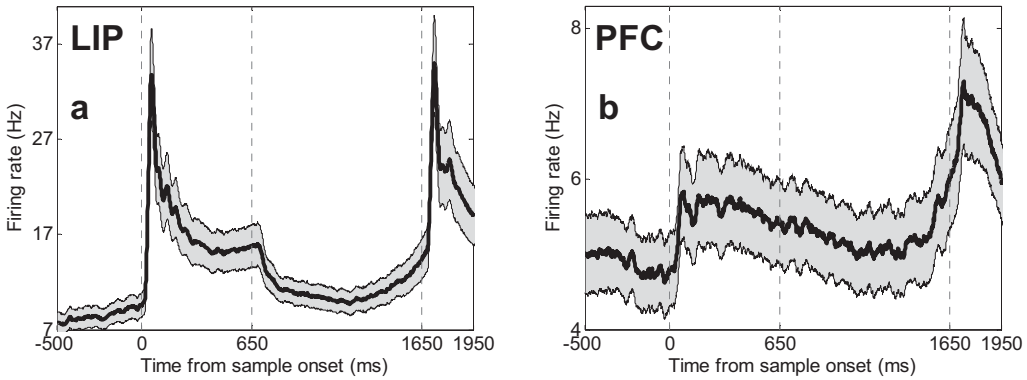

Figure S4. **Average firing rates across LIP and PFC populations.** Traces show the average firing rates across all neurons that were direction selective (according to one-way ANOVA at $P < 0.01$) during any epoch in (a) LIP (N=67) and (b) PFC (N=155) using a 35 ms smoothing window. The shaded gray area around the solid traces indicates the standard error of the mean.

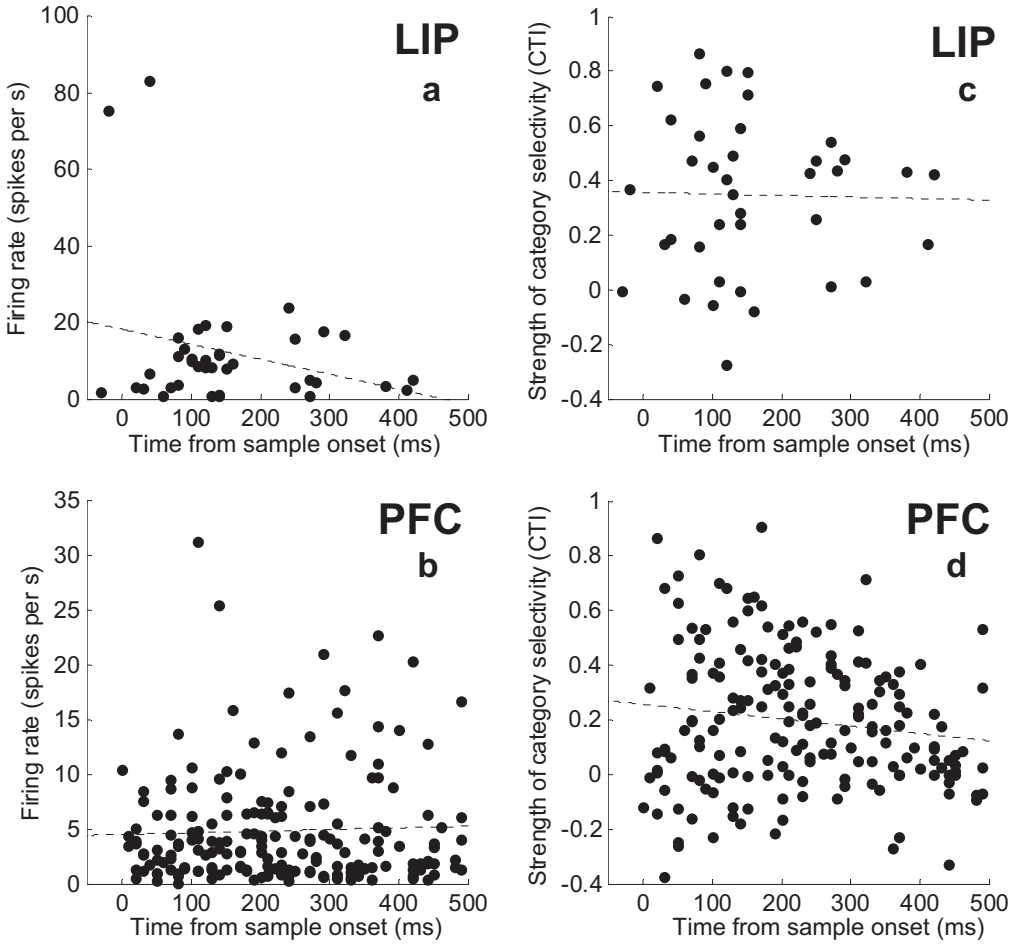

Figure S5. Relationship of category selectivity latency with category selectivity strength and firing rate. (a,b) Scatter plots show the relationship between firing rate and category selectivity latency for LIP (a) and PFC (b) neurons using the category tuning index based latency measure. (c,d) Scatter plots show the relationship between category selectivity strength and category selectivity latency for LIP (c) and PFC (d) neurons using the category tuning index based measure. For panels a-d, linear regression fits are indicated by the dotted line.

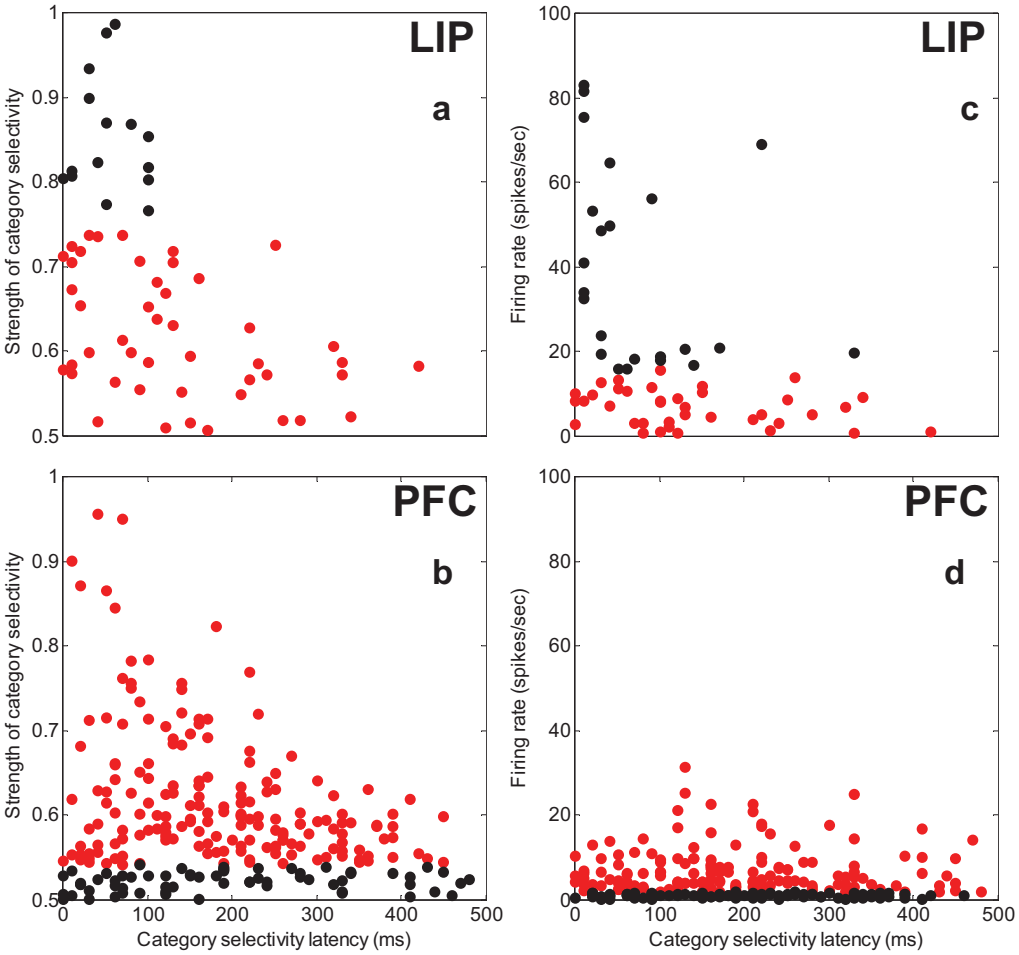

Figure S6. Controls for the relationship of category selectivity latency with category selectivity strength and firing rate. (a,b) The ROC value and latency of category selectivity is shown for all neurons included in the ROC latency analysis described in the main manuscript. The black points indicate neurons that were excluded in the latency control analyses in the supplemental info. The populations of LIP (a) and PFC (b) neurons in red have the same average category index value. (c,d) The average firing rate (during 80-500 ms after sample onset) and latency of category selectivity is shown for all neurons included in the ROC latency analysis described in the main manuscript. The black points indicate neurons that were excluded in the latency control analyses in the supplementary info. The populations of LIP (c) and PFC (d) neurons in red have the same average firing rate.

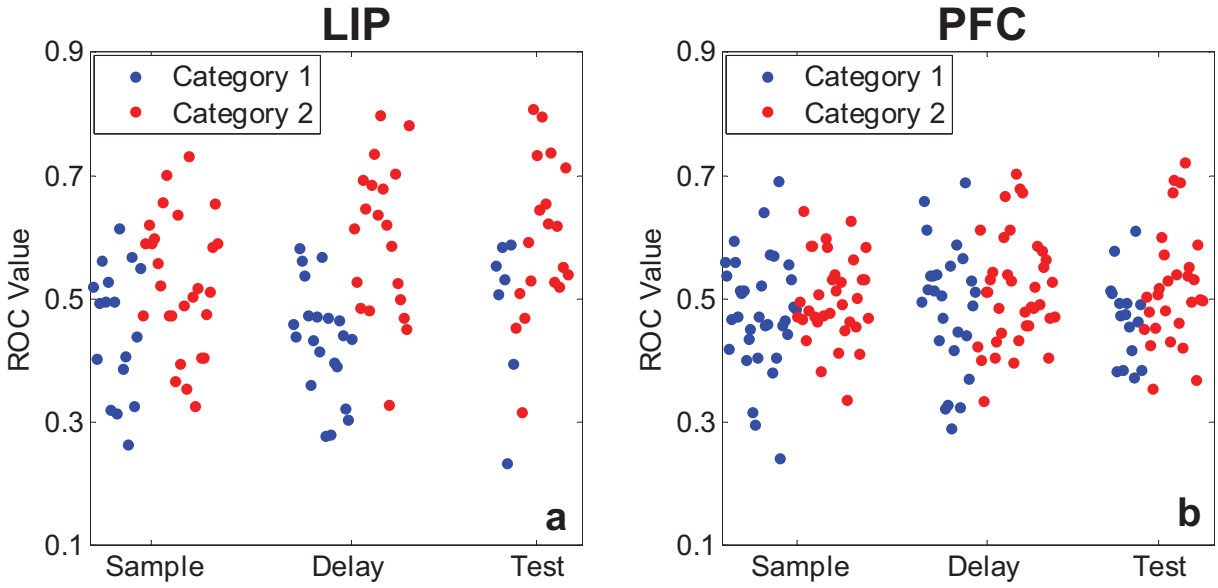

Figure S7. Category selectivity on ambiguous boundary trials. Each point on the scatter plots indicates the ROC value (comparing activity on Category 1 and Category 2 trials) of an individual LIP (a) or PFC (b) neuron on ambiguous boundary trials during the sample, delay, or test epochs. ROC values of 0.0 and 1.0 indicate strong selectivity for Category 1 and Category 2, respectively, on ambiguous trials (sorted according to the monkeys' classification on each trial). Neurons' category preferences on non-ambiguous trials are indicated by the color of each point (blue=Category 1; red=Category 2). All direction selective neurons (according to a one-way ANOVA at $P<0.01$) in each epoch are shown. This is the same data used to compute the mean values shown in Figs. 5e,f.